Computational Modelling of Wire Biosensor with Competitive Substrates Conversion

Vytautas Ašeris *Member, IAENG*

***Abstract*—Glucose biosensors are analytical devices used mainly for the recognition of glucose in blood. A wire biosensor utilizing a competitive substrates conversion is analysed in this paper. Two substrates (oxygen and glucose) are competing over the single enzyme (*Aspergillus niger glucose oxidase*) in the analysed reactions. However, oxygen concentration is not of any importance in this case and it is considered as disturbance. The purpose of this work was to define the parameter values of the biosensor, at which oxygen concentration does not affect the response of the biosensor. The behaviour of the biosensor is defined by the mathematical model with reaction-diffusion equations of non-linear type. The suggested mathematical model is solved numerically, by using finite difference technique, as the analytical solutions exist only for a very few selected cases because of the non-linearity in the reaction term. The simulations showed complex biosensor dynamics at various values of enzymatic membrane thickness and concentration. The calibration curves signifying the effective range of the biosensor operation were provided.**

***Index Terms*—Biosensor, modelling, competitive substrates conversion, glucose, oxygen.**

I. Introduction

BIOSENSORS are reliable sensing devices used for the detection of a specific substance (substrate) in the analysed solution [1]. During the biosensor action, biosensor-specific product appears which is detected and transmitted to the biosensor output device with a help of transducer element. According to the transducer type, biosensors are classified into electrochemical, electrical, optical, piezoelectric, thermometric [2]. Various biosensors are constantly being developed and applied in point-of-care testing, home diagnostics, environmental monitoring, research laboratories, process industry, security and biodefense and others [3], [4]. In the medical field, a majority of biosensors are included in glucose meters, blood gas analysers, electrolyte analysers, metabolite analysers and various drug detectors [1], [5], [6], [7].

The creation of new biosensors or the optimization of the existing ones by means of physical experiments is troublesome and tedious process. Part of the experiments can be replaced by using mathematical modelling [8], [9]. In most cases a biosensor is modelled as a reaction-diffusion system [4]. However, such systems usually include non-linear reaction term, which complicates the solving of the model, as the exact analytical solutions exist only for a specific set of parameter values [10]. To simulate biosensor operation in wide ranges of parameter values a digital simulations are employed [11].

Manuscript received March 14, 2014; revised April 09, 2014. This research is funded by the European Social Fund under the Global Grant measure, Project No. VP1-3.1-ŠMM-07-K-01-073/ MTDS-110000-583.

V. Ašeris, PhD, is with the Department of Software Engineering, Faculty of Mathematics and Informatics, Vilnius University, LT-08303, Vilnius. e-mail: vytautas.aseris@mif.vu.lt.

Glucose biosensors occupy more than 85% of all the biosensor market [12]. This type of biosensor is a compact instrument with an exceptional technology for the accurate and rapid diagnoses of blood glucose level. Various glucose biosensors were developed and analysed by using mathematical modelling as long as since 1976 [13]. Consideration of insulin "age structure" for modelling blood glucose dynamics is analysed in [14]. The dual use of horseradish peroxidase and glucose oxidase for the glucose biosensor is analysed in [15]. The effect of membrane permeability and selectivity on the performance of such sensor is analysed in [16].

A layer by layer assembling of the biosensor model is common for various biosensors, including glucose sensors [17]. The same approach is applied in this work to build the mathematical model of the wired biosensor. Biosensor with competitive substrates conversion in this work is modelled and targeted as the glucose detection sensor. Two substrates - glucose and oxygen - are capable of binding with one of the more common and relatively cheap enzymes analysed in this paper - *Aspergillus niger glucose oxidase*. However, only the detection and recognition of glucose is important. The purpose of this work was to analyse biosensors behaviour numerically and to define the configuration of the biosensor, at which the influence of the oxygen concentration is minimal.

II. Properties of the biosensor

Physical biosensor is considered as a system consisting of wire electrode, which is covered with enzyme layer. The cross-section of this bioelectrode is displayed in Fig. 1. Enzyme (*Aspergillus niger glucose oxidase*) reacts with oxygen and glucose in the cyclic reaction:

$$\mathrm{E_{ox}} + \mathrm{Glucose} \longrightarrow \mathrm{E_{red}} + \delta\text{-glucolactone}, \qquad (1)$$

$$\mathrm{E_{red}} + \mathrm{O_2} \longrightarrow \mathrm{E_{ox}} + \mathrm{H_2O_2}. \qquad (2)$$

In the terms of substrates and product the reaction scheme (1-2) can be written as follows:

$$\mathrm{E_{ox}} + \mathrm{S_{gl}} \underset{k_{-1}}{\overset{k_1}{\rightleftharpoons}} \mathrm{ES} \xrightarrow{k_2} \mathrm{E_{red}} + \mathrm{P_1}, \qquad (3)$$

$$\mathrm{E_{red}} + \mathrm{S_o} \xrightarrow{k_3} \mathrm{E_{ox}} + \mathrm{P}, \qquad (4)$$

where $\mathrm{E_{ox}}$, $\mathrm{E_{red}}$ and ES stand for the oxidized enzyme, the reduced enzyme and the enzyme-substrate complex, respectively, P and $\mathrm{P_1}$ are the reaction products, similarly as in [18]. The large difference of the timescales [19] in the reaction network (3) and (4) creates difficulties for simulating the temporal evolution of the network and for understanding

ISBN: 978-988-19253-5-0
ISSN: 2078-0958 (Print); ISSN: 2078-0966 (Online)

the basic principles of the biosensor operation. To sidestep these problems, the QSSA is often applied [20], [21],

$$\frac{\partial e_{ox}}{\partial t} \approx \frac{\partial e_{red}}{\partial t} \approx \frac{\partial e_s}{\partial t} \approx 0. \quad (5)$$

where e_{red}, e_{ox} and e_s, are the molar concentrations of the oxidized enzyme $\mathrm{E_{ox}}$, the reduced enzyme $\mathrm{E_{red}}$ and the enzyme-substrate complex ES, respectively. By applying the quasy-steady state assumption as it is defined in (5), the total reaction rate v can be expressed as follows:

$$v = \frac{e_0 k_{cat} k_{red} k_{ox} s_{gl}^{(2)} s_o^{(2)}}{k_{red} k_{ox} s_{gl}^{(2)} s_o^{(2)} + k_{cat} k_{ox} s_o^{(2)} + k_{cat} k_{red} s_{gl}^{(2)}}, \quad (6)$$

where $s_{gl}^{(2)}$ and $s_o^{(2)}$ are the concentrations of glucose and oxygen, respectively, e_0 is the total concentration of enzyme in the enzymatic membrane, $k_{cat} = k_2$ is catalytic constant of ES conversion, $k_{red} = k_1 k_2/(k_{-1} + k_2)$ is an apparent bimolecular constant of the enzyme and substrate interaction, $k_{ox} = k_3$ is a constant of the enzyme interaction with the mediator [22]. The notation of (2) denotes the layer number, in which the concentration is measured (the second layer is the enzymatic membrane, see Fig. 1).

III. Mathematical model

The biosensor is considered as a thin wire electrode covered with the enzyme layer. A Nernst diffusion layer is considered outside the electrode-enzyme system (see Fig. 1). Since the electrode is much larger in length compared with its diameter, we describe the mathematical model in one dimensional space, which includes the following regions:

1) An electrode ($l = 1, a_0 < r < a_1$), where no processes take place. At the boundary of a_1 the electrons are collected. The radius of this layer is $d_0 = a_1 - a_0$.
2) The enzyme layer ($l = 2, a_1 < r < a_2$) where the biochemical reactions (3) and (4) as well as the mass transport by diffusion takes place. The radius of this layer is $d_1 = a_2 - a_1$.
3) A diffusion limiting region ($l = 3, a_2 < r < a_3$), where only the mass transport by diffusion takes place. This layer was modelled according to the Nernst approach [9], [1]. The radius of this layer is $d_3 = a_3 - a_2$.
4) A convective region ($r > a_3$), where the substrate concentration is maintained constant. Convective region is considered to be much larger in volume than the bioelectrode system, therefore it's thickness is not defined.

A. Governing equations

No biochemical processes are present in the electrode ($a_0 < r < a_1$) and the concentrations of all substances are always equal to zero ($t > 0$),

$$c^{(1)}(r,t) = 0, \quad c = s_{gl}, s_o, p, \quad (7)$$

where r and t stand for the space (as a distance from the electrode at $a_0 = 0$) and time, respectively, $s_{gl}^{(1)}(r,t)$, $s_o^{(1)}(r,t)$, $p^{(1)}(r,t)$ are the molar concentrations of the glucose $\mathrm{S_{gl}}$, oxygen $\mathrm{S_o}$ and product P respectively.

By coupling the reaction kinetics described in the previous section with the mass transport by the diffusion, we form the following reaction-diffusion type equations for the enzymatic membrane ($a_1 < r < a_2$, $t > 0$):

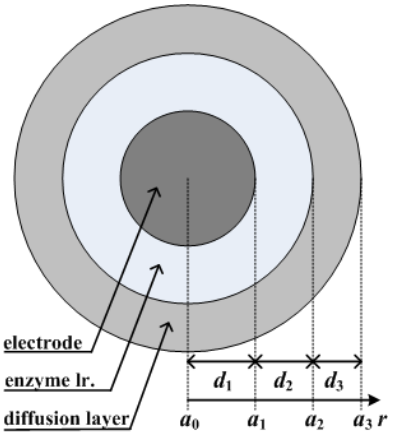

Fig. 1. A cross-section of the electrode

$$\frac{\partial s_{gl}^{(2)}}{\partial t} = D_{s_{gl}}^{(2)} \left(\frac{\partial^2 s_{gl}^{(2)}}{\partial r^2} + \frac{1}{r} \frac{\partial s_{gl}^{(2)}}{\partial r} \right) - v, \quad (8a)$$

$$\frac{\partial s_o^{(2)}}{\partial t} = D_{s_o}^{(2)} \left(\frac{\partial^2 s_o^{(2)}}{\partial r^2} + \frac{1}{r} \frac{\partial s_o^{(2)}}{\partial r} \right) - v, \quad (8b)$$

$$\frac{\partial p^{(2)}}{\partial t} = D_p^{(2)} \left(\frac{\partial^2 p^{(2)}}{\partial r^2} + \frac{1}{r} \frac{\partial^2 p^{(2)}}{\partial r^2} \right) + v, \quad (8c)$$

where $s_{gl}^{(2)}(r,t)$, $s_o^{(2)}(r,t)$, $p^{(2)}(r,t)$ are the molar concentrations of the glucose $\mathrm{S_{gl}}$, oxygen $\mathrm{S_o}$ and product P respectively, $D_{s_{gl}}^{(2)}$, $D_{s_o}^{(2)}$, $D_p^{(2)}$ are the diffusion coefficients of corresponding substances in the enzyme layer. All forms of enzyme are considered to be immobilized, and therefore there are no diffusion terms in the corresponding equations. The reaction product $\mathrm{P_1}$ has no influence to the biosensor response and therefore it is not described in the mathematical model.

Outside of the enzyme layer only the mass transport by diffusion of glucose, oxygen and product takes place (enzyme is considered to be non-diffusive). It was assumed that the external mass transport obeys a finite diffusion regime ($t > 0, a_2 < r < a_3$),

$$\frac{\partial c^{(3)}}{\partial t} = D_c^{(3)} \left(\frac{\partial^2 c^{(3)}}{\partial r^2} + \frac{1}{r} \frac{\partial c^{(3)}}{\partial r} \right), \quad c = s_{gl}, s_o, p, \quad (9)$$

where $s_{gl}^{(3)}(r,t), s_o^{(3)}(r,t)$ and $p^{(3)}(r,t)$ stand for the molar concentrations of the glucose, oxygen and product in the diffusion layer, $D_{s_{gl}}^{(l)}, D_{s_o}^{(l)}$ and $D_p^{(l)}$ are the diffusion coefficients of glucose, oxygen and product in the diffusion layer, which is treated as the Nernst diffusion layer [9]. According to the Nernst approach the thickness $d_3 = a_3 - a_2$ remains unchanged with time. Away from it ($r > a_3$) the buffer solution is in motion and uniform in concentration.

B. Initial conditions

The biosensor operation starts when substrates appear in the bulk solution ($t = 0$) and is described for the enzymatic

ISBN: 978-988-19253-5-0
ISSN: 2078-0958 (Print); ISSN: 2078-0966 (Online)

($l = 2$) and diffusion ($l = 3$) layers,

$$c^{(l)}(r,0) = 0, \quad c = s_{gl}, s_o, p, \quad a_{l-1} < r < a_l, \tag{10a}$$

$$s_{gl}^{(2)}(a_1,0) = 0, \qquad s_{gl}^{(3)}(a_3,0) = s_{0,gl}, \tag{10b}$$

$$s_o^{(2)}(a_1,0) = 0, \qquad s_o^{(3)}(a_3,0) = s_{0,o}, \tag{10c}$$

$$p^{(2)}(a_1,0) = 0, \qquad p^{(3)}(a_3,0) = 0, \tag{10d}$$

where $s_{0,gl}$ and $s_{0,o}$ are the concentrations of the glucose and oxygen, respectively, in the bulk solution, l is the layer number according to the numbering in Fig. 1.

C. Boundary and matching conditions

During the biosensor operation the concentrations of the glucose, oxygen and product in the bulk solution remain constant, as the bulk solution is considered to be much larger in volume compared to the analysed biosensor system. The concentration $p^{(2)}$ of the reaction product at the electrode surface ($r = a_1$) is being permanently reduced to zero due to the electrode polarization. Following the scheme (3)-(4), the substrate is an electro-inactive substance. This is described by the following boundary conditions ($t > 0$):

$$D_c^{(2)} \frac{\partial c^{(2)}}{\partial r}\bigg|_{r=a_1} = 0, \quad c^{(3)}(a_3,t) = c_0, \quad c = s_{gl}, s_o, \tag{11a}$$

$$p^{(2)}(a_1,t) = 0, \quad p^{(3)}(a_3,t) = 0. \tag{11b}$$

On the boundary between two adjacent regions having different diffusivities, the matching conditions are defined ($t > 0$),

$$D_c^{(2)} \frac{\partial c^{(2)}}{\partial r}\bigg|_{r=a_2} = D_c^{(3)} \frac{\partial c^{(3)}}{\partial r}\bigg|_{r=a_2}, \quad c = s_{gl}, s_o, p, \tag{12a}$$

$$c^{(2)}(a_2,t) = c^{(3)}(a_2,t), \qquad c = s_{gl}, s_o, p. \tag{12b}$$

These conditions mean that fluxes of the glucose, oxygen and product from enzymatic membrane are considered to be equal to the corresponding fluxes entering the surface ($r = a_2$) of the diffusion layer and vice versa. The partition coefficients of both substrates and product in between enzymatic and diffusion layers are considered to be equal and therefore are not introduced in the mathematical model.

D. Biosensor response

The electric current is measured as a response of the biosensor in a physical experiment. The density $i(t)$ of the current at time t is proportional to the gradient of the product P concentration p at the electrode surface ($r = a_1$) and is obtained according to Fick's and Faraday's laws [5],

$$i(t) = n_e F D_p^{(2)} \frac{\partial p^{(2)}}{\partial r}\bigg|_{r=a_1}, \tag{13}$$

where F is Faraday's constant ($F = 96.485 \times 10^6$ $\mathrm{CM^{-1}m^{-3}}$), n_e is a number of electrons involved in the electrochemical reaction.

Mathematical model approaches the steady-state as $t \to \infty$,

$$i_s = \lim_{t\to\infty} i(t). \tag{14}$$

TABLE I
CONSTANT PARAMETER VALUES OF THE BIOSENSOR MODEL.

Description	Notation	Value	Dimen.
Nernst diffusion layer thickness	d_3	5×10^{-5}	m
Diffusion coefficient of glucose in the dialysis membrane	$D_{s_{gl}}^{(2)}$	3.4×10^{-11}	$\mathrm{m^2 s^{-1}}$
Diffusion coefficient of glucose in the diffusion layer	$D_{s_{gl}}^{(3)}$	6.3×10^{-10}	$\mathrm{m^2 s^{-1}}$
Diffusion coefficient of oxygen in the dialysis membrane	$D_{s_o}^{(2)}$	1.4×10^{-9}	$\mathrm{m^2 s^{-1}}$
Diffusion coefficient of oxygen in the diffusion layer	$D_{s_o}^{(3)}$	2.12×10^{-9}	$\mathrm{m^2 s^{-1}}$
Diffusion coefficient of product in the dialysis membrane	$D_p^{(2)}$	3.1×10^{-10}	$\mathrm{m^2 s^{-1}}$
Diffusion coefficient of product in the diffusion layer	$D_p^{(3)}$	1.4×10^{-9}	$\mathrm{m^2 s^{-1}}$
Reaction rate of catalytic constant of ES conversion	k_{cat}	8.8×10^2	$\mathrm{M^{-1}}$
Reaction rate of the enzyme and glucose interaction	k_{red}	1.2×10^4	$\mathrm{M^{-1} s^{-1}}$
Reaction rate of the enzyme interaction with the oxygen	k_{ox}	1.5×10^6	$\mathrm{M^{-1} s^{-1}}$
Number of electrodes	n_e	1	-

TABLE II
CHANGED PARAMETER VALUES OF THE BIOSENSOR MODEL.

Description	Notation	Interval	D.
Radius of the electrode	d_1	$[5 \times 10^{-5}; 5 \times 10^{-4}]$	m
Enzyme layer thickness	d_2	$[10^{-5}; 10^{-4}]$	m
Glucose concentration	$s_{0,gl}$	$[10^{-3}; 2 \times 10^{-2}]$	M
Oxygen concentration	$s_{0,o}$	$[5.5{\times}10^{-5}; 2.74{\times}10^{-4}]$	M
Enzyme concentration	e_0	$[10^{-7}; 10^{-4}]$	M

IV. DIGITAL SIMULATION

In general case, a presented mathematical model can be solved numerically with analytical solutions existing only for a specific set of parameter values [9], [10]. In our investigation we used the finite difference method by introducing a uniform grid in space (with a total of number of 800 points) and time directions. An explicit finite difference scheme has been built to solve a problem [8], [11]. The software of the digital simulator has been programmed in C++ language. In the digital simulation the steady state time t_r was assumed when the change of the current is relatively small during the relatively large time,

$$t_r = \min_{i(t)>0} \left\{ t : \frac{t}{i(t)} \left| \frac{di(t)}{dt} \right| < \varepsilon \right\}, \quad i(t_r) \approx i_s. \tag{15}$$

The decay rate ε highly influences the response time: when $\varepsilon \to 0$, $t_r \to \infty$. In our calculations we used $\epsilon = 10^{-3}$.

A. Parameter values

The constant values of the parameters used in the digital investigation process are provided in Table I. The remaining model parameters were changed as described in Table II.

ISBN: 978-988-19253-5-0
ISSN: 2078-0958 (Print); ISSN: 2078-0966 (Online)

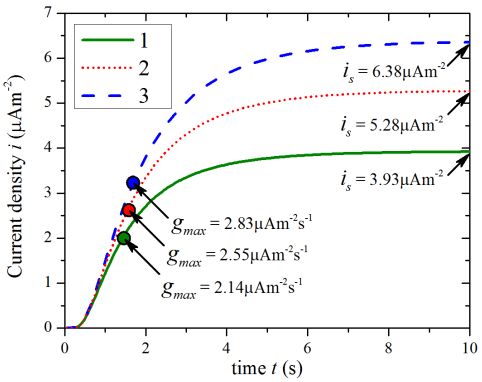

Fig. 2. Biosensor response in time at three different concentrations of oxygen s_o: 6.85×10^{-5} (1), 1.37×10^{-4} (2) and 2.74×10^{-4}M (3). Electrode radius was $d_1 = 5 \times 10^{-5}$m, enzymatic membrane thickness was $d_2 = 10^{-5}$m. Other parameter values as defined in Table I.

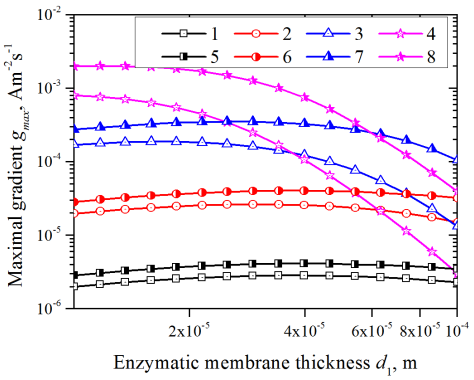

Fig. 3. Maximal gradient of the current versus enzymatic membrane thickness at four different values of enzyme concentration e_0: $10^{-7}(1,5), 10^{-6}(2,6), 10^{-5}(3,7), 10^{-4}(4,8)$M and at two different concentrations of oxygen $s_{0,o}$: 5.5×10^{-5}(1-4), 2.74×10^{-4}(5-8)M. Radius of the electrode was $d_1 = 5 \times 10^{-5}$m. Other parameter values were as defined in Table I.

B. Model validation

By increasing the radius of the electrode, the mathematical model described in this paper approaches the model used in [22], which is described in Cartesian space. By using $d_1 = 0.01$m and by changing the other parameter values as defined in Table II, the relative current difference between the model described in this work and the one described in [22] was less than 1%.

Additionally, validation of concentrations was carried out by checking if the concentration values do not contain any sudden spikes in the inner sections of the layers.

The solution starts by applying initial conditions at time moment $t = 0$. Mesh points at the initial time row are calculated according to the discretized initial conditions of the mathematical model. Time step is increased, and new row of the concentration values is calculated according to the approximated governing, boundary and matching conditions. When the concentrations for all the compounds at all mesh points of the new time step are calculated, validation of the concentrations is executed.

If the validation of concentrations does not fail (as it is a mandatory requirement), the calculations are continued. If they fail, the time step is decreased repeatedly, while the time step reaches such size, that the calculations would proceed long enough without any failure for the condition (15) to be satisfied.

C. Biosensor response

Biosensor response in time at three different glucose concentrations s_o (6.85×10^{-5}, 1.37×10^{-4}, 2.74×10^{-4}M) of oxygen is displayed in Fig. 1. Electrode radius was $d_1 = 5 \times 10^{-5}m$, enzymatic membrane thickness was $d_2 = 10^{-5}m$. Other parameter values were the same as defined in Table I.

As one can see from Fig. 2, the response i is monotonically increasing function of time t. By increasing oxygen concentration four times from $s_{0,o} = 6.85 \times 10^{-5}$M (curve 1) to $s_{0,o} = 2.74 \times 10^{-4}$M (curve 3), the steady state response increases from $i \approx 3.93\mu$A to $i \approx 6.38\mu$A (an increase of 62.3%). Such a large sensitivity to the concentration of oxygen is unsuitable when constructing real life glucose biosensors. By measuring the maximal gradient of the current as the response, as it is defined in (16), the biosensor sensitivity to oxygen can be reduced,

$$g_{max} = \max_{t>0} \frac{di(t)}{dt}. \tag{16}$$

In the analysed case, a quadruple increase in oxygen concentration increases the maximal gradient value only by 32.2% (from $2.14 \times 10^{-6}\mu As^{-1}$ in curve 1 to $2.83 \times 10^{-6}\mu As^{-1}$ in curve 3) - approximately two times lower relative difference than in case of the steady state current. The use of maximal gradient value instead of the steady state current is perspective in another point of view, as the final measured response is reached several times faster - a result attractive when designing medical biosensors. Therefore, in all the following simulations we used maximal gradient value (16) as the final response of the biosensor instead of the steady state response (14).

V. Results

A. The influence of enzymatic membrane

Enzymatic membrane thickness is known to be very important when designing new biosensors [3], [4]. The impact of the enzyme membrane thickness d_2 at four different concentrations e_0 ($10^{-7}, 10^{-6}, 10^{-5}, 10^{-4}$M) of enzyme is displayed in Fig. 3. The calculations were carried out at two different concentrations of oxygen (minimum value of $s_{0,o} = 5.5 \times 10^{-5}$M and maximum value of $s_{0,o} = 2.74 \times 10^{-4}$M), while other parameter values were as defined in Table I.

When enzyme concentration is relatively low ($e_0 \leq 10^{-6}$M, curves 1 and 5, 2 and 6, Fig. 3), the maximal gradient of the current is non-monotonic function of d_2. However, the non-monotonicity is not of high magnitude, and the relative difference between the responses for different oxygen concentrations at these enzyme concentrations are virtually identical. However, the mentioned relative difference increases for the larger enzymatic sensitivities ($e_0 \geq 10^{-5}$M, curves 3 and 7, 4 and 8) - the largest relative difference between two responses for different oxygen concentrations is more than tenfold ($d_2 = 10^{-4}$m, curves 4 and 8, Fig. 3). The conclusion can be made, that the smallest possible enzymatic membrane thickness corresponds to the smallest sensitivity to oxygen concentration.

ISBN: 978-988-19253-5-0
ISSN: 2078-0958 (Print); ISSN: 2078-0966 (Online)

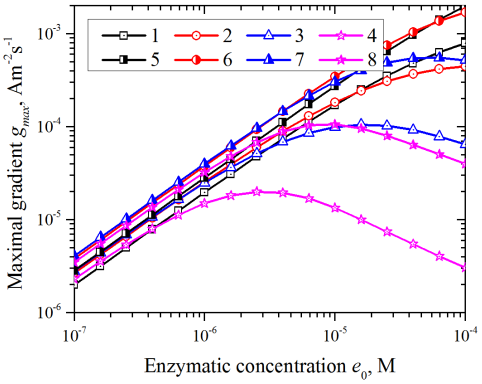

Fig. 4. Maximal gradient of the current versus the enzyme concentration at four different values of enzymatic membrane thickness d_2: $10^{-5}(1,5), 2.16\times10^{-5}(2,6), 4.65\times10^{-5}(3,7)$ and $10^{-4}(4,8)$m and at two different concentrations of oxygen $s_{0,o}$: 5.5×10^{-5}(1-4), 2.74×10^{-4}(5-8)M. Electrode radius was $d_1 = 5\times10^{-5}$m. Other parameter values were as defined in Table I.

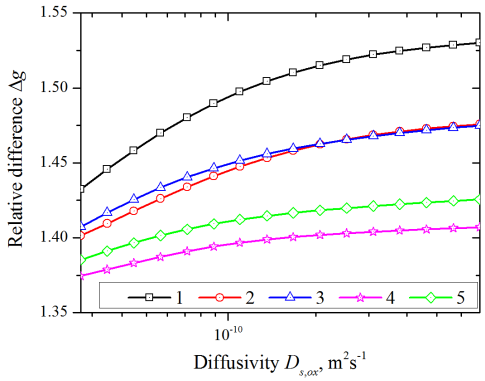

Fig. 5. Oxygen increase versus diffusivity of glucose in the enzymatic membrane at five different combinations of oxygen and product diffusivities: $D^{(2)}_{sg}$: $1.4\times10^{-10}(1,2), 5\times10^{-10}(5), 2.12\times10^{-9}(3,4)$m^{2}s^{-1} and $D^{(2)}_{p}$: $3.1\times10^{-11}(1,3), 2\times10^{-10}(5), 1.4\times10^{-9}(2,4)$m^{2}s^{-1}. Radius of the electrode was $d_1 = 5\times10^{-5}$m, enzymatic membrane thickness $d_2 = 10^{-5}$m, enzyme concentration $e_0 = 10^{-7}$M. Other parameter values were as defined in Table I.

As it was noticed in Fig. 3, the enzyme concentration e_0 has a high impact on the biosensor response as well as sensitivity to oxygen concentration. Therefore, the impact of the enzymatic concentration on the biosensor response is analysed in Fig. 4 at four different enzyme membrane thicknesses d_2 ($10^{-5}, 2.16\times10^{-}5, 4.65\times10^{-5}$ and 10^{-4}m). The boundary values of the oxygen concentration were the same as in Fig. 3, all the other parameter values as defined in Table I.

For the relatively small enzymatic membrane thicknesses ($d_2 < 3\times10^{-5}$m, curves 1 and 5, 2 and 6, Fig. 4), the maximal gradient of the current is steadily increasing function of enzymatic concentration e_0. However, for the larger enzymatic membrane thickness ($d_2 > 3\times10^{-5}$m, curves 3 and 7, 4 and 8), the response decreases with an increase of enzymatic concentration. However, the smallest difference between two responses for different oxygen concentrations is at the smallest values of enzymatic concentration ($e_0 = 10^{-7}$M). The enzymatic membrane thickness affects the influence of enzymatic concentration on the response - the larger enzymatic membrane thickness corresponds to the larger difference between the responses of different oxygen concentration. The smallest enzymatic membrane thickness (curves 1 and 5, Fig. 4) corresponds for the smallest sensitivity to oxygen concentration - a result reaffirming the results displayed in Fig. 3. At $e_0 = 10^{-7}$M and $d_0 = 10^{-5}$m, the response of $g_{max} = 1.99\times10^{-6}\mu$A$s^{-1}$ at the smallest oxygen concentration ($s_{0,o} = 5.5\times10^{-5}$M) and the response of $g_{max} = 2.83\times10^{-6}\mu$A$s^{-1}$ at the largest oxygen concentration ($s_{0,o} = 2.74\times10^{-4}$M) is the smallest (relative difference being 42%). Therefore, in all the following calculations we use the value $d_2 = 10^{-5}$m for the enzymatic membrane thickness and the value $e_0 = 10^{-7}$M for the enzyme concentration.

B. The impact of the diffusivity

The sensitivity to oxygen concentration can be decreased down to 42%, however, the diffusivity can be employed to further eliminate the influence of oxygen. The impact of the diffusion coefficient $D^{(2)}_{sgl}$ on the sensitivity to oxygen concentration at various values of $D^{(2)}_{s_o}$ and $D^{(2)}_{p}$ is analysed in Fig. 5. The value of $D^{(2)}_{sgl}$ was changed between tenfold smaller than the one provided in Table I and up to the value of $D^{(3)}_{sgl}$. At the largest value of $D^{(2)}_{sgl}$, the glucose would diffuse through the boundary of $r = a_2$ without any resistance. The parameters of $D^{(2)}_{s_o}$ and $D^{(2)}_{p}$ were changed in the similar manner. The impact of oxygen is measured as the following ratio:

$$\Delta g = g_{max}(s_{o,max})/g_{max}(s_{o,min}), \qquad (17)$$

where $g_{max}(s_{o,max})$ and $g_{max}(s_{o,min})$ stand for the responses of the biosensor at maximum ($s_{0,o} = 2.74\times10^{-4}$M) and minimum ($s_{0,o} = 5.5\times10^{-5}$M) concentrations of oxygen. The best previously determined values of enzymatic membrane thickness ($d_2 = 10^{-5}$m) and enzyme concentration ($e_0 = 10^{-7}$M) were used, while other parameter values were as defined in Table I.

As one can see from Fig. 5, the impact of oxygen is monotonically increasing function of $D^{(2)}_{sgl}$. The dynamics of oxygen impact are virtually identical at the smallest ratio (curve 2) and largest ratio (curve 3) between $D^{(2)}_{s_o}$ and $D^{(2)}_{p}$. The impact of oxygen is largest, when the diffusion coefficients $D^{(2)}_{s_o}$ and $D^{(2)}_{p}$ are smallest (curve 1). The smallest values of oxygen impact are achieved at the largest values of $D^{(2)}_{s_o}$ and $D^{(2)}_{p}$ (curve 4) - meaning that oxygen and product would diffuse through the boundary of $r = a_2$ without resistance. The smallest overall value of $\Delta g = 1.37$ is obtained at $D^{(2)}_{sgl} = 3.4\times10^{-11}$m^{2}s^{-1} (curve 4).

C. Calibration curves

Calibration curves are employed for development of the real-life biosensors, as they are pre-programmed in the electronic parts of these devices [1], [6]. The impact of the response on the glucose concentration at three different electrode radius sizes d_1 ($5\times10^{-6}, 10^{-5}, 5\times10^{-5}$m) and two boundary oxygen concentrations $s_{0,o}$ (5.5×10^{-5}M and $s_{0,o} = 2.74\times10^{-4}$M) is displayed in Fig. 6. The parameters were $D^{(2)}_{sgl} = 3.4\times10^{-11}$m^{2}s^{-1}, $D^{(2)}_{s_o} = 2.12\times10^{-9}$m^{2}s^{-1}, $D^{(2)}_{p} = 1.4\times10^{-9}$m^{2}s^{-1}, $d_2 = 10^{-5}$m, $e_0 = 10^{-7}$M. Other parameter values were as defined in Table I.

The parameter values defined for the lowest impact of oxygen concentration correspond to appropriate calibration

ISBN: 978-988-19253-5-0
ISSN: 2078-0958 (Print); ISSN: 2078-0966 (Online)

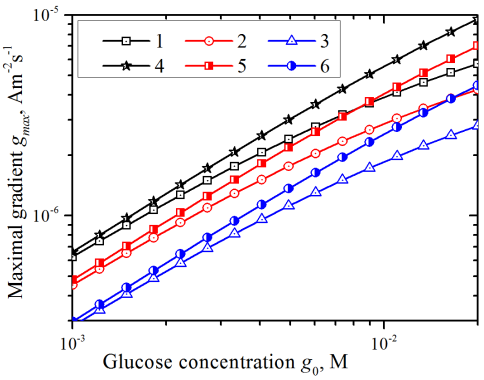

Fig. 6. Maximal gradient of the current versus the glucose concentration at three different values of electrode radius d_1: $10^{-5}(1,4), 5 \times 10^{-5}(2,5), 10^{-4}(3,6)$m and two different values of oxygen $s_{0,o}$: 5.5×10^{-5}(1-3), 2.74×10^{-4}(4-6)M. Other parameters were $D_{s_{gl}}^{(2)} = 3.4 \times 10^{-11}\text{m}^2\text{s}^{-1}$, $D_{s_o}^{(2)} = 2.12 \times 10^{-9}\text{m}^2\text{s}^{-1}$, $D_p^{(2)} = 1.4 \times 10^{-9}\text{m}^2\text{s}^{-1}$, $d_2 = 10^{-5}$m, $e_0 = 10^{-7}$M and as in Table I.

curves, as all of them are almost linear (see Fig. 6). Linear calibration curve corresponds to excellent biosensor sensitivity to glucose, meaning that the change in glucose concentration corresponds to the respective change in biosensor response. The impact of oxygen concentration is decreased to minimum, when comparing with previous analysis. The smallest impact of oxygen is for the smallest concentrations of glucose. The radius of the electrode practically does not influence the impact of oxygen, however the radius has a reverse impact on the biosensor response: the smaller radius corresponds to the larger values of the response (curves 1 and 4) and vice versa (curve 3 and 6).

VI. Conclusion

The mathematical model provided in this paper can be successfully used for digital simulation of glucose biosensor behaviour. The impact of oxygen concentration on the biosensor response can be decreased by using the following recommendations:

1) Use maximal gradient of the response instead of the steady state response, which provides better response times and lower oxygen impact.
2) Smallest enzymatic membrane thickness and smallest enzyme concentrations are recommended, as they decrease oxygen impact by 5 times, approximately.
3) The smallest possible diffusion coefficient of glucose and the largest possible diffusion coefficients of oxygen and product in the enzymatic membrane correspond to the further decrease (by approximately 15%) of oxygen impact.

By following these recommendations a more sensitive to glucose biosensor can be developed by using *Aspergillus niger glucose oxidase* as enzyme.

Acknowledgment

Author thanks to the research group of ”Biomoda” in Vilnius University for the valuable discussions regarding the computational modelling of biosensors. The help from professors Romas Baronas and Juozas Kulys from Vilnius University are greatly appreciated.

References

[1] F. Scheller and F. Schubert, *Biosensors*. Amsterdam, Netherlands: Elsevier, 1992.
[2] R. Monošík, M. Stredanský, and E. Šturdík, “Biosensors - classification, characterization and new trends,” *Acta Chimica Slovaca*, vol. 5, no. 1, pp. 109–120, Jan. 2012.
[3] J. D. Newman and S. J. Setford, “Enzymatic biosensors,” *Molecular Biotechnology*, vol. 32, no. 3, pp. 249–268, Mar. 2006.
[4] A. Sadana and N. Sadana, *Handbook of biosensors and biosensor kinetics*. Amsterdam, Netherlands: Elsevier, 2010.
[5] F. Scheller and J. Fedrowitz, *Frontiers in Biosensorics*, ser. EXS (Basel). Birkhauser Varloy, 1997.
[6] J. Cooper and A. Cass, *Biosensors: A Practical Approach*, 2nd ed., ser. Practical Approach Series No 268. Oxford, UK: Oxford University Press, 2004.
[7] A. P. Turner, I. Karube, and G. S. Wilson, *Biosensors: fundamentals and applications*, ser. Oxford science publications. Oxford, UK: Oxford University Press, 1987.
[8] R. Baronas, F. Ivanauskas, and J. Kulys, *Mathematical Modeling of Biosensors*, 1st ed., ser. Springer Series on Chemical Sensors and Biosesnsors. Dordrecht, Netherlands: Springer, Apr. 2010.
[9] D. Britz, *Digital Simulation in Electrochemistry*, 3rd ed., ser. Lecture Notes in Physics. Berlin, Germany: Springer Berlin Heidelberg, 2005.
[10] T. Schulmeister, “Mathematical modelling of the dynamic behaviour of amperometric enzyme electrodes,” *Selective Electrode Reviews*, vol. 12, no. 2, pp. 203–260, 1990.
[11] A. A. Samarskij, *The theory of difference schemes*. New York, New York, USA: Marcel Dekker, 2001.
[12] G. I. A. Inc., “Biosensors in Medical Diagnostics - a Global Strategic Business Report,” Global Industry Analysts, Inc., Tech. Rep., 2012.
[13] L. D. Mell and J. Maloy, “Amperometric response enhancement of the immobilized glucose oxidase enzyme electrode,” *Analytical Chemistry*, vol. 48, no. 11, pp. 1597–601, Sep. 1976.
[14] A. Cambiaso, L. Delfino, M. Grattarola, G. Verreschia, D. Ashworth, A. Maines, and P. Vadgama, “Modelling and simulation of a diffusion limited glucose biosensor,” *Sensors and Actuators B: Chemical*, vol. 33, no. 1-3, pp. 203–207, 1996.
[15] D. Mackey, A. J. Killard, A. Ambrosi, and M. R. Smyth, “Optimizing the ratio of horseradish peroxidase and glucose oxidase on a bienzyme electrode: Comparison of a theoretical and experimental approach,” *Sensors and Actuators B: Chemical*, vol. 122, no. 2, pp. 395–402, Mar. 2007.
[16] A. Abd. Aziz, “Mathematical Modeling Of An Amperometric Glucose Sensor: The Effect Of Membrane Permeability And Selectivity On Performance,” *Jurnal Teknologi*, vol. 51, no. 1, pp. 77–94, Dec. 2009.
[17] R. A. Croce Jr., S. Vaddiraju, F. Papadimitrakopoulos, and F. C. Jain, “Theoretical Analysis of the Performance of Glucose Sensors with Layer-by-Layer Assembled Outer Membranes,” *Sensors*, vol. 12, no. 10, pp. 13 402–13 416, Oct. 2012.
[18] V. Ašeris and R. Baronas, “Using GRID Computing to Model Biosensors Acting in Stirred and Non-Stirred Solutions,” in *Proceedings of the 5th European Conference on Computational Fluid Dynamics (ECCOMAS CFD 2010)*, C. F. Pereira, A. Sequeira, and J. M. C. Pereira, Eds., Lisbon, Portugal, 2010, pp. 14–17.
[19] N. Čenas and J. Kulys, “Biocatalytic oxidation of glucose on the conductive charge transfer complexes,” *Bioelectrochemistry and Bioenergetics*, vol. 8, no. 1, pp. 103–113, 1981.
[20] L. A.Segel and M. M. Slemrod, “The Quasi-Steady-State Assumption: A Case Study in Perturbation,” *SIAM Review*, vol. 31, no. 3, pp. 446–477, Sep. 1989.
[21] B. Li, Y. Shen, and B. Li, “Quasi-steady-state laws in enzyme kinetics,” *The Journal of Physical Chemistry. A*, vol. 112, no. 11, pp. 2311–2321, Mar. 2008.
[22] R. Baronas and J. Kulys, “Modelling Amperometric Biosensors Based on Chemically Modified Electrodes,” *Sensors*, vol. 8, no. 8, pp. 4800–4820, Aug. 2008.

ISBN: 978-988-19253-5-0
ISSN: 2078-0958 (Print); ISSN: 2078-0966 (Online)